Performance Analysis of Ultra Wideband Multiple Access Time Hopping – Pulse Shape Modulation in Presence of Timing Jitter

D. Adhikari* and C. Bhattacharya

Symbiosis Institute of Technology, Pune-412 115, India
Defence Institute of Advanced Technology, Pune-411 025, India
E-mail: adhikaridebashis@gmail.com

ABSTRACT

In short-range networks such as wireless personal area networks (WPAN), multiple user wireless connectivity for surveillance would require a wireless technology that supports multiple streams of high-speed data and consumes very little power. Ultra wideband (UWB) technology enables wireless connectivity across multiple devices (users) addressing the need for high-speed WPAN. Apart from having a distinct advantage of higher data rate over Bluetooth v4.0 (24 Mbps), the UWB technology is also found to be tolerant to frequency-selective multipath fading. In this paper authors discuss a time-hopping pulse shape modulation UWB signalling scheme for ad-hoc high bit rate wireless connectivity for defence applications. Authors analyse multiple access interference for both Gaussian channel and frequency selective multipath fading channel to compare the effects of timing jitter on two types of pulse shapes, namely modified Hermite pulse (MHP) and prolate spheroidal wave functions (PSWF). Authors make a comparative analysis of the system performance with respect to PSWF and MHP to ascertain robustness to timing jitter. In the process, authors introduced a new metric of decision factor in timing jitter analysis.

Keywords: Multiple access, ultra wideband, Hermite pulse, time-hopping pulse shape modulation

1. INTRODUCTION

Short-range wireless communication and ad-hoc networking can provide a device level wireless connectivity for battlefield monitoring and surveillance purposes. Such secured connectivity in wireless personal area networks (WPAN) needs to support multiple streams of high data rate (>100 Mbps), should consume very little power, and maintain low cost while sometimes fitting into a very small physical package[1]. Traditional wireless technology cannot meet these requirements. This has motivated an unprecedented development of ultra wideband (UWB) technology.

The UWB radio technology is baseband transmission of sub-nanosecond pulses offering high bandwidth. It is an emission technique with very low transmitted power level over short communication ranges (< 10 m). Due to the availability of wide bandwidth and high resolution in time UWB signalling systems are very robust to interferences and multipath distortions. UWB thus offers a distinct advantage in having wireless connectivity with high data rates across multiple devices for WPAN applications (IEEE 802.15.4a) that make it suitable for defence applications.

However, the advantages of UWB system in terms of reduced complexity and robustness to multipath fading are constrained due to utilisation of highly narrow pulses[2]. This arises due to the effects of timing jitters, tracking errors and unstable clocks[3] with jitter of 10 ps reported by Rowe[4], *et al.* The relative mobility between transmitter and receiver adds to the asynchronisation problem. Immediate fallout of timing jitter is performance degradation of correlation receiver, resulting in reduction of signal-to-noise ratio (*SNR*)[5-7]. The effects of timing jitter on the bit error rate (BER) performance and data throughput for wireless body area network (WBAN) were compared for equally correlated-pulse position modulation (PPM) scheme in Nasr & Shaban[8]. A built in jitter measurement principle using tail fitting methods for jitter analysis is presented in Erb & Pribyl[9]. Analysis of a time hopping - pulse position modulation (TH-PPM) scheme in presence of timing jitter for a multipath fading channel is discussed in Gezici[10].

An indoor ad-hoc WPAN scenario is considered with multiple access connectivity between few sources (N_u users, say User 1 represents a navigation map, User 2 represents a data control information and so on.) and is shown in Fig. 1. This information available in the form of *M*-ary symbols at the cockpit of an aircraft is required to be accessed through a wireless channel by a helmet-mounted receiver of the pilot, forming an indoor WPAN scenario.

The underlying idea in a time-hopping pulse shape modulation (TH-PSM) scheme is to represent these *M*-ary symbols $a_i = [a_{i0}, a_{i1,\dots}, a_{i,k-1}]$ with a set of *K* orthogonal pulses $\psi_k(t)$, $\Psi = [\psi_0, \psi_{1,\dots}, \psi_{(k-1)}]$ as basis functions[11-12]. The ith symbol for the nth user will therefore be

$$s_i^{(n)}(t) = \sum_{k=0}^{K-1} a_{i,k}^{(n)} \psi_k(t) \tag{1}$$

The signal from each of the N_u users is superimposed to form a composite transmitted signal for a dense multiple access
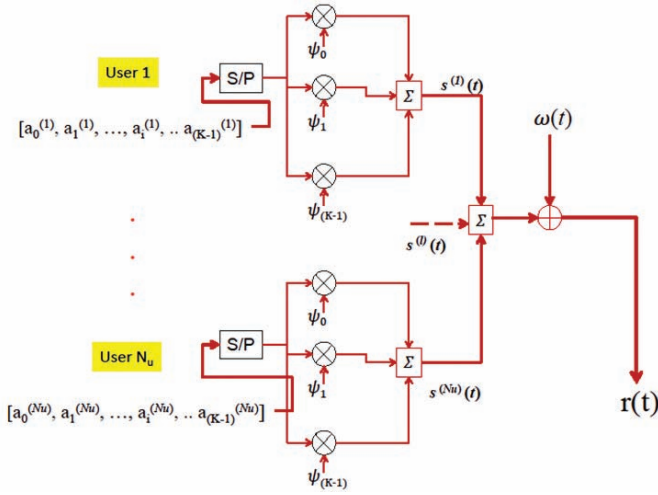
Figure 1. System model for TH-PSM scheme.

environment. In Fig. 1, $r(t)$ is the composite received signal and $\omega(t)$ is the additive white Gaussian noise (AWGN). The advantage of *M*-ary PSM scheme is the requirement of less timing precision, better immunity to multipath and independence of the received signal polarity during detection[13]. It is proposed for achieving high data rates even in severe multipath fading scenarios[11].

In this paper, authors discussed TH-PSM scheme for ad-hoc high bit rate wireless connectivity for multiple devices. The aim of this paper is performance comparison of the TH-PSM scheme with respect to two UWB pulse shapes, namely modified Hermite pulses (MHP) and prolate spheroidal wave functions (PSWF) for ascertaining the system robustness to timing jitter. The analysis is done for dense multiple access environments for an AWGN channel as well as for a frequency-selective multipath environment. A new metric decision factor (D_f) was introduced to determine the tolerance to timing jitter for both the pulse shapes. It was also demonstrated the effect of timing jitter on the signal to interference and noise ratio (SINR) and bit error probability (BEP).

2. SYSTEM MODEL FOR TIME-HOPPING PULSE SHAPE MODULATION SCHEME

The message symbol from each user is mapped onto *K* orthogonal ($M=2^K$) pulse shapes $\psi_k(t)$. Since a single orthogonal set of pulses representing a symbol does not provide enough information the user data is modulated onto a parallel sequence of pulse shapes over N_f frames as shown in Fig. 2. However, continuous pulse transmission leads to strong spectral lines in the spectrum of the transmitted signal[14]. These energy spikes may interfere with other communication systems over short distances. To minimise such interferences, a randomising technique in the form of time hopping is applied to the transmitted signal that makes the transmission more noise like[15] thereby making the system secure.

The transmitted signal for the ith symbol of the nth user as shown in Fig. 2. is

$$s_i^{(n)}(t) = \sqrt{E_{tr}} \sum_{j=1}^{N_f} \sum_{k=0}^{K-1} a_{i,k}^{(n)} \psi_k(t - jT_f - c_j^{(n)} T_c - \varepsilon) \qquad (2)$$

where $a_i = [a_{i0}, a_{i1,...}, a_{i,k-1}]$ is the *K*-tuple representation for the ith symbol $i \in \{0, 1,.., M\text{-}1\}$. The frame time duration is T_f, ε is the timing jitter at the transmitter modelled as uniformly distributed random variable $U[-\varepsilon, \varepsilon]$[8]. Transmitted energy E_{tr} is ideally the same for a perfect power control and T_c is the time slot for each UWB pulse. Total number of slots per frame is N_c where $T_{f=} N_c T_c$, and the total number of frames to represent a symbol is N_f. In a multiple access scenario, the transmitted pulses from many users may arrive at the receiver simultaneously. To avoid catastrophic collision due to such probable simultaneous arrival of received pulses, each pulse is made to occupy a particular slot in a frame in a random manner depending on a pseudorandom (PN) code $c_j^{(n)}$, $(0 < c_j \leq N_c\text{-}1)$ that is explained in Fig. 2.

3. RECEIVED SIGNAL IN A MULTIPLE ACCESS SCENARIO IN GAUSSIAN CHANNEL

The composite received signal from each of N_u users with AWGN $\omega(t)$ is
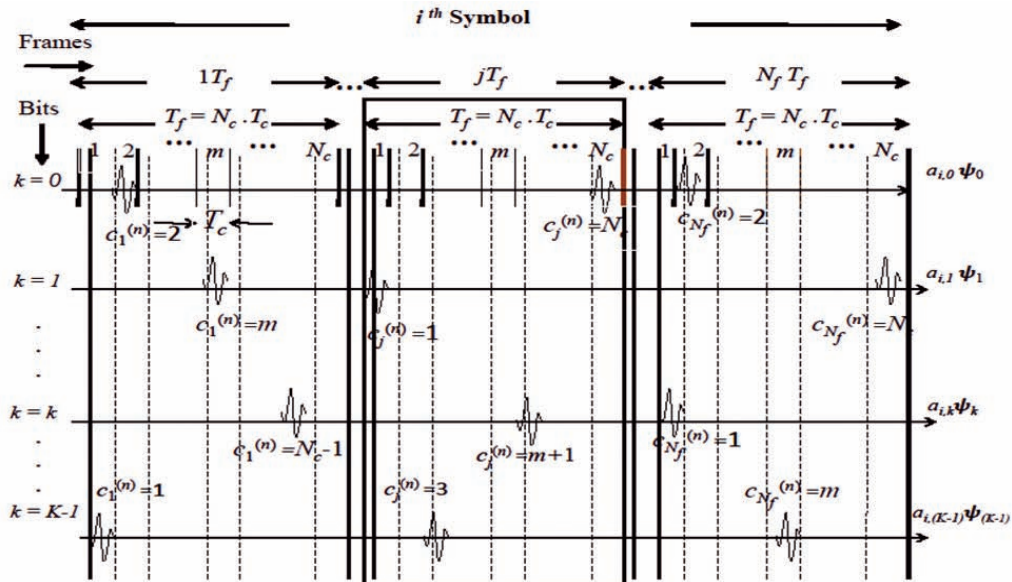

Figure 2. Schematic representation of *M* – ary TH-PSM scheme.

$$r(t) = \sum_{n=0}^{N_u-1} \sqrt{E_{tr}} \sum_{j=1}^{N_f} \sum_{k=0}^{K-1} a_{i,k}^{(n)} \psi_k(t - jT_f - c_j^{(n)} T_c - \varepsilon) + \omega(t)$$

(3)

The *SINR* for the ith symbol of the desired lth user in a multiple access PSM scenario is

derived as $$SINR = \frac{\sqrt{E} \sum_{k=0}^{K-1} \sum_{j=1}^{N_f} a_i^{(l)} \varphi_{(l,l)}(\varepsilon)}{\sqrt{\sigma_{MAI}^2 + \sigma_{\omega}^2}}$$

(4)

Here, $\varphi_{(l,l)}(\varepsilon)$ is the autocorrelation function (ACF) between the template and received signal of the desired lth user

$$\varphi_{(l,l)}(\varepsilon) = \int_{-\infty}^{\infty} \psi_l(t)\psi_l(t-\varepsilon)d\varepsilon,$$

(5)

σ_{MAI}^2 is the variance due to multiple access interference and σ_{ω}^2 is the variance due to AWGN.

3.1 Multiple Access Interference

The sum of interferences to each frame of the lth correlator (template for the desired user) due to signal from user n ($n \neq l$) is given as Z_{MAI} and is shown in Fig. 3 for a single frame of transmission.

$$Z_{MAI} = \sum_{n=0,n\neq l}^{N_u-1} \sqrt{E_{tr}} \sum_{j=1}^{N_f} \sum_{k=0}^{K-1} a_i^{(n)} \int_{-\infty}^{\infty} \psi_l(t)\psi_l(t-\varepsilon)d\varepsilon$$

(6)

Depending upon the value of $c_i^{(l)}$ the template would occupy one of the slots out of $[1, 2, ..., N_c]$ for each bit in a frame of the lth user. Based upon the magnitude of the timing jitter an overlap of pulses will occur. Cross-correlation for other users ($n \neq l$) with the template of the lth user would exist only for those slots. Probable interferences between the template for the kth bit of ith symbol of the desired (lth) user and received kth bit of the undesired user ($n \neq l$) are provided in the following cases and is also depicted in Fig. 3.

Case I - For slots $T_c \in [2,...., N_c-1]$: The correlation between ith symbol of the nth user and template of lth user refers to a situation when both the pulses are of the same slot and the overlap is only due to the delay difference in timing jitter. Also

Figure 3. Schematic representation of probable cases of MAI.

there is an overlaying of the template pulse with adjacent slots within the same frame due to jitter delay ($\pm\varepsilon$).

Case II- For slot $T_c = 1$: In this case correlation between the kth bit of $(i$-$1)$th symbol of the nth user and desired lth user template would result due to an overlap of $(T_c + \varepsilon)$ for $(i$-$1)$th symbol of the nth user and the ith symbol of the template. The overlap of the kth bit of $(i+1)$th symbol of the undesired user and the ith symbol of the template is similarly due to $(T_c - \varepsilon)$.

Case III- For slot $T_c = N_c$: This is similar to Case II except that the correlation is now between ith or $(i+1)$th symbol of the nth user and desired lth user template.

The total *MAI* is the sum of interference of the above cases for each of $(N_u - 1)$ users. Assuming the *MAI* and the noise to be approximately Gaussian distributed, we obtain the mean *MAI* as

$$E[Z_{MAI}] = \frac{1}{2N_c}\left\{E[\varphi(\varepsilon)] + E[\varphi(T_c - |\varepsilon|)]\right\} = \frac{\gamma_1}{2N_c}$$

(7)

The variance is calculated as

$$\sigma_{MAI}^2 \approx \frac{2N_c-1}{4N_c^2}\gamma_1^2 + \frac{N_c-1}{2N_c^2}\gamma_2 + \frac{1}{N_c}\gamma_3$$

(8)

where

$$\gamma_1 = E[\varphi(\varepsilon)] + E[\varphi(T_c - |\varepsilon|)]$$

(9a)

$$\gamma_2 = E[\varphi^2(T_c - |\varepsilon|)]$$

(9b)

$$\gamma_3 = E[\varphi(\varepsilon)\varphi(T_c - |\varepsilon|)]$$

(9c)

Each of N_u users in a PSM scheme utilise different sets of orthogonal basis functions $\psi(t)$ so that $\varphi_{n,l}(\varepsilon) \approx 0$ in Eqn. (4). Also large values of N_c in Eqn. (7) results in smaller σ_{MAI}^2. The average *BEP* for a wireless communications system being inversely proportional to the *SINR*, a large value of $\varphi_{i,j}(\varepsilon)$ along with a smaller value of σ_{MAI}^2 would yield a smaller average *BEP*. Consequently, correct estimation of the ith symbol is governed by the area under $\varphi_{n,l}(\varepsilon)$.

4. RECEIVED SIGNAL IN A MULTIPATH CHANNEL FOR MULTIPLE ACCESS SCENARIO

The authors adopted a discrete multipath channel model in a frequency-selective environment whose impulse response $h(t)$ is

$$h(t) = \sum_{l=0}^{L-1} \alpha_l \delta(t - \tau_l)$$

(10)

where α_l and τ_l are the fading coefficients and the corresponding multipath delay for the lth path respectively. We assume that the minimum path time resolution is equal to the pulse-width $T_p (T_p \approx T_c)$ such that the multipath components arrive at some integer multiple of T_p, i.e., $\tau_l = lT_p$. We also assume that multipath components are mutually uncorrelated and considering closely spread users in an indoor environment the number of multipath components to be the same (L) for each user. The fading coefficients representing the path loss α_l follow a probability density function as specified in IEEE 802.15.4a channel model and is applicable in the 2 GHz - 10 GHz frequency range.
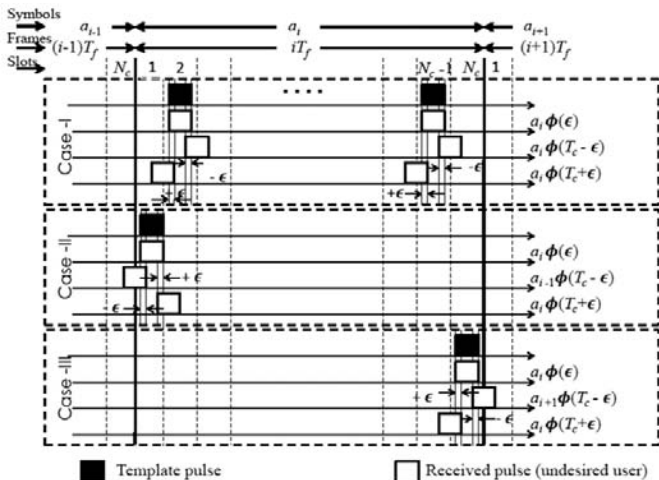
The composite received signal from all N_u users for the ith symbol with L path components is

$$r(t) = \sum_{n=0}^{N_u-1} \sum_{l=0}^{L-1} \alpha_l s_i^{(n)}(t - lT_p) + \omega(t) \tag{11}$$

In a multiuser scenario with L copies of received signal for each transmitted signal due to multipath, one needs a co-channel demodulation for simultaneous detection of all signals. The authors adopted a RAKE combiner[16] with the assumption that the reference or template waveform is perfectly synchronised with the desired signal. The template for the kth bit correlator of the nth user with L branches representing as many multipath components is

$$\Psi_k(t) = \sum_{p=0}^{L-1} \beta_p^{(n)} \psi_k(t - jT_f - c_j^{(n)}T_c - pT_p) \tag{12}$$

where $\beta_p^{(n)}$ is the RAKE combining coefficient for the pth branch of the RAKE combiner. The delay pT_p is introduced to synchronise for the delay due to the pth multipath. The delay spread of the channel is assumed to be not larger than the frame time T_f, i.e, $L \le N_c T_c$.

The pth branch template of the RAKE combiner represents the pulse-shape corresponding to the kth bit of PSM from the transmitter delayed by $\tau_p = pT_p$. The composite received signal $\Psi_k(t) = \sum_{p=0}^{L-1} \beta_p^{(n)} \psi_k(t - jT_f - c_j^{(n)}T_c - pT_p)$, consists of multiple copies of pulses from all N_u users due to multipath effects. The decision statistics at the correlator output of the pth branch template for the desired user ($n = 1$) is

$$y(t) = \int_{jT_f}^{(j+1)T_f} r(t)\psi_k(t - pT_p)dt = \sum_{n=0}^{N_u-1} \sqrt{E_{tr}} \sum_{k=0}^{K-1} \sum_{j=1}^{N_f} \sum_{l=0}^{L-1} \alpha_l^{(n)} \beta_p^{(1)} \left\langle a_{i,k}^{(n)}, \varphi_{kp}(\tau_k) \right\rangle \tag{13}$$

where

$$\varphi_{(l,l)}(\varepsilon) = \int_0^{T_f} \psi_k(t - lT_p - \varepsilon)\psi_p(t - pT_p)dt \tag{14}$$

and the random delay τ_k represents the delay difference between the incoming signal due multipath and timing jitter delays and the template, $\tau_k = [(l - p)T_p + \varepsilon]$.

4.1 Determination of SINR in a Multipath-Multiple Access Scenario

The correlation between the pth - branch template for the kth bit of the desired user ($n = 1$) with the composite received signal $r(t)$ may lead to the following probable cases in the receiver and are described in Fig. 4.

Case I: Assuming perfect synchronisation, the lth multipath component of the kth bit of the desired user is autocorrelated with those of the template ($l = p$) yielding the desired signal component, Z_{DES}.

Case II: The lth multipath component of the kth bit in the jth frame of the desired user spill over to the adjacent $(j+1)^{th}$ frame due to multipath and timing jitter, and overlap with the pth branch template of the same order in the $(j+1)^{th}$ frame resulting in inter-frame interference, Z_{IFI}.

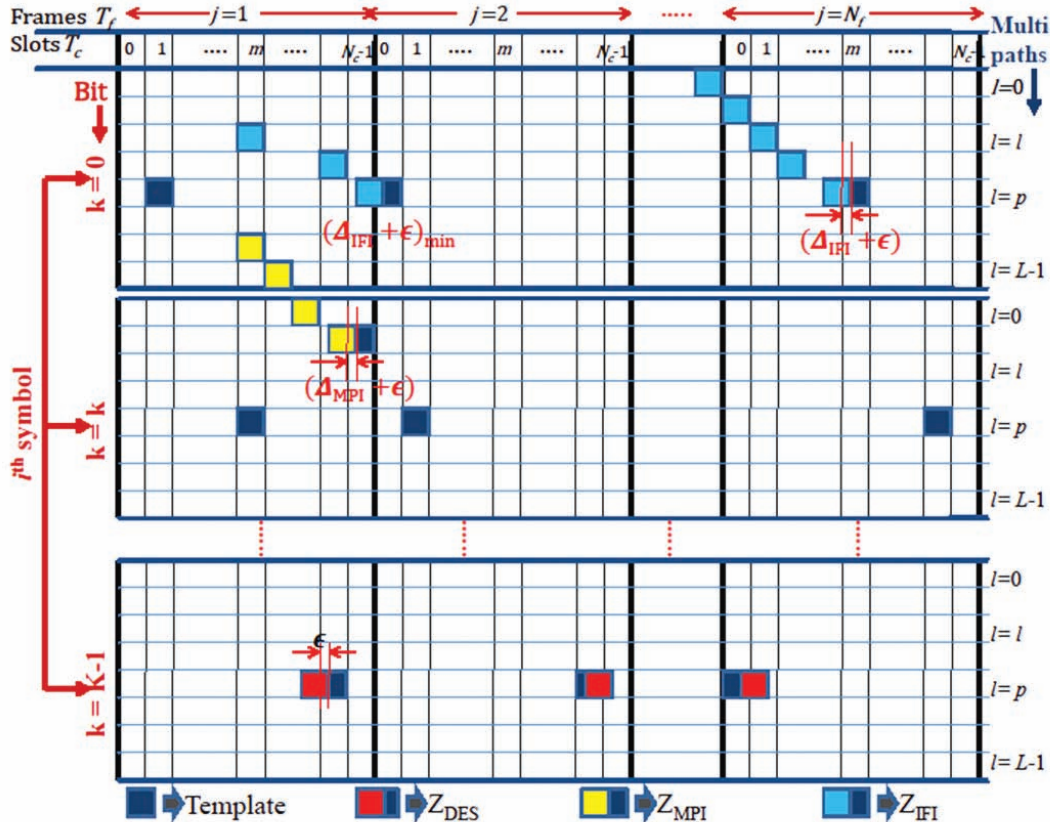*Case III:* Some of the multipath components of the kth bit of

Fig. 4 Pulse correlation between p^{th} branch template of kth bit with composite received signal.

467

the desired user would interfere with the qth ($\neq k$) bit of the template causing multi-pulse interference, Z_{MPI}

Case IV: The sum of interference to each frame of the pth correlator branch of the kth pulse due to signal from other users (N_u-1) is given as the multiple access interference, Z_{MAI}

The decision statistics in Eqn. (13) terms of desired signal and the interferences is

$$y(t) = Z_{DES} + Z_{IFI} + Z_{MPI} + Z_{MAI} + Z_\omega \tag{15}$$

and Z_ω is the interference due to AWGN.

The *SINR* for multiple access scenario in a multipath environment is given as

$$SINR = \frac{(Z_{DES})^2}{(\sigma_{IFI}^2 + \sigma_{MPI}^2 + \sigma_{MAI}^2 + \sigma_\omega^2)} \tag{16}$$

The probability of error for the pth correlator branch of the kth bit is the BEP and is given by

$$P_p = Q\left(\sqrt{\frac{E_{tr}[\sum_{j=1}^{N_f} \alpha_l^{(1)}\beta_p^{(1)}\varphi_{kk}(\varepsilon)]^2}{(\sigma_{IFI}^2 + \sigma_{MPI}^2 + \sigma_{MAI}^2 + \sigma_\omega^2)}}\right) \tag{17}$$

Selection of mutually exclusive set of orthogonal pulses for different users reduces σ_{MPI}^2 and σ_{MAI}^2 significantly. However, the effect of σ_{IFI}^2 is not negligible.

5. DETERMINATION OF TOLERANCE TO JITTER BY DECISION FACTOR METRIC

Probability of error in Eqn. (17) is found to be dependent on the auto- and cross-correlation functions between the received and the template pulses. To yield a smaller value for average *BEP*, a large value of ACF $\varphi_{kk}(\varepsilon)$ for the desired signal and a smaller value of variance σ_{IFI}^2 due to interferences is desirable. Consequently, correct estimation of the kth bit in the ith symbol is governed by the area under $\varphi_{kk}(\varepsilon)$. Since the magnitude of $\varphi_{kk}(\varepsilon)$ goes down with higher amount of delay due to timing jitter ε, an upper-bound of timing jitter (ε_{th}) is estimated corresponding to a threshold value of $\varphi_{kk}(\varepsilon_{th})$. This corresponds to a value of *SINR* below which the detector would estimate a bit erroneously.

We define a decision factor D_f in Z_{DES} as the ratio of the overlapping area under the ACF due to the received pulse with jitter above ε_{th} of the desired user ($n = 1$) to the total area under the ACF. Since for Z_{DES}, $l = p$ resulting in $\tau_k = \varepsilon$, one obtains

$$D_f = \left.\frac{\int_{\varepsilon_{th}}^{\infty} \varphi_{kk}(\varepsilon)d\varepsilon}{\int_0^{\infty} \varphi_{kk}(\varepsilon)d\varepsilon}\right|_{Z_{DES}} \tag{18}$$

ACF being an even symmetrical function.

In the worst case scenario, the *SINR* becomes minimum when the contribution due to Z_{IFI} is maximum. For such a case

SINR at the pth branch of the kth bit correlator in terms of D_f may be expressed as

$$SINR = \frac{\sqrt{E_{tr}^{(1)}} N_f D_f (\alpha_l^{(1)}\beta_p^{(1)}) \int_0^{\infty} \varphi_{kk}(\varepsilon)d\varepsilon}{\sqrt{E_{tr}^{(1)} A^2 E[\varphi_{kk}^2 \{(N_c - 2) + \varepsilon\}] + \sigma_\omega^2}} \tag{19}$$

where

$$A = (N_f - 1)(L - 1)\left[\frac{(N_c - m)(m)}{N_c^2}\right](\alpha_l^{(1)}\beta_p^{(1)}) \tag{20}$$

As the system model parameters E_{tr}, N_c, N_f, T_f, and L remain the same and the multipath channel impulse response being independent of the pulse shape, the system performance for TH-PSM with respect to *SINR* effectively depends on the pulse shape parameters, D_f and $\varphi_{kk}(\varepsilon)$.

6. RESULTS AND ANALYSIS OF SINR FOR PSWF AND MHP PULSE SHAPES

For analysing the performance of TH-PSM scheme in presence of timing jitter MHP and PSWF pulse shapes since these pulse shapes were considered exhibit the property of orthogonality and optimally utilizes the restrictions imposed by FCC regulated spectral mask[17]. Due to its unique property of double orthogonality in time and frequency representations and spectral efficiency, PSWF pulses are an attractive option[18]. With an additional degree of freedom in terms of time-bandwidth product 'c' besides pulse shape order 'n', one has the option for selecting a larger set of basis functions with PSWF pulse shapes.

MHP and PSWF pulse shapes of width T_p = 2 ns, orders $n = 2$, 4, and 6 and time bandwidth product $c = 2$, 4, and 6 have been considered. The normalised ACF plot for PSWF (in black color) and MHP (in red colour) with $n = 6$, $c = 6$ is shown in Fig. 5. In the Fig. 5 $\varphi(\varepsilon_{th})$ implies the value of ACF at a timing jitter of ε_{th}. The timing jitter threshold ε_{th} for each order is taken as 10, 20 and 40 picosecs. The decision factor metric D_f evaluated for PSWF and MHP pulse shapes for different jitter delays is shown in Table 1. From Fig. 5 and Table 1, it is observed that

- For the same order of pulse shape n, $D_{f(PSWF)}$ is greater than $D_{f(MHP)}$. This indicates that *SINR* for PSWF will always be greater than MHP for all orders of pulse shapes as is evident from Eqn. (19).

- For the same value of ε_{th}, $\varphi(\varepsilon_{th})_{PSWF}|_{\varepsilon_{th}} \ggg \varphi(\varepsilon_{th})_{MHP}|_{\varepsilon_{th}}$ implying higher value of *SINR* for PSWF compared to MHP. This result is shown in Fig. 5 for $n = 6$ and $c = 6$ where $\varphi(40p\sec s)_{PSWF} = 0.7498$ and $\varphi(40p\sec s)_{MHP} = 0.2903$ for $\varepsilon_{th} = 40p\sec s$. Hence for similar jitter conditions, the detection of symbols mapped by PSWF pulse shapes is better than those mapped with MHP pulses.

- For the same value of $\varphi(\varepsilon_{th})$, ε_{th} is larger for PSWF pulse shapes than for MHP. This implies that for the same *SINR*, the TH-PSM signaling scheme-based on PSWF can demonstrate better tolerance to timing jitter. From above, it was conclude that the upper-bound of timing jitter for better *SINR* is larger for PSWF than for MHP pulse shapes. The reason for such behaviour can be attributed
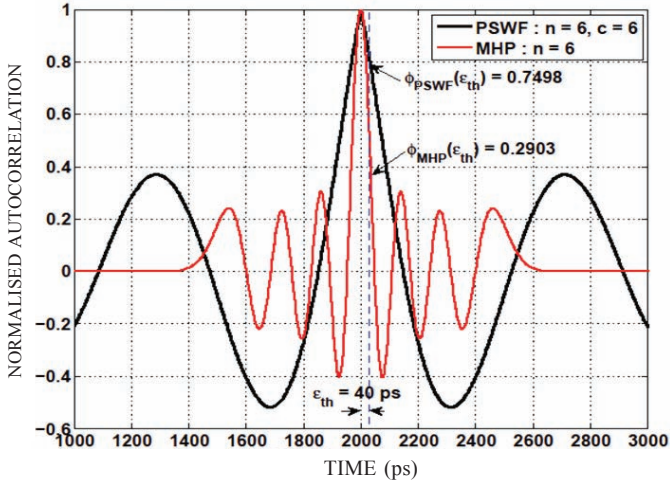
Figure 5. ACF plots for MHP and PSWF of order $n = 6$ and $c = 6$.

Table 1. Decision factor (D_f) for MHP and PSWF

n	(ps)	MHP	PSWF $c = 2$	$c = 4$	$c = 6$
	10	0.79147	0.95192	0.95685	0.95956
2	20	0.59222	0.90497	0.91429	0.91927
	40	0.25855	0.81452	0.81451	0.81443
	10	0.72284	0.91437	0.91092	0.91637
4	20	0.46772	0.83265	0.82577	0.83561
	40	0.10399	0.68107	0.66768	0.68340
	10	0.67025	0.87877	0.87509	0.87436
6	20	0.37806	0.76566	0.75845	0.75196
	40	0.03122	0.56394	0.55054	0.53333

to the smaller de-correlation time for MHP compared to PSWF for the same pulse width.

The variation *SINR* and *BEP* as given in Eqns (17) and (19) in terms of D_f is simulated with the following parameters: $N_c = 10$, $N_f = 3$, $L = 10$, $\alpha_l = 0.5817$ and $\sigma_\omega^2 = 0.001$. The effect of timing jitter on *SINR* and *BEP* for both PSWF and MHP is shown in Figs 6 - 7. It was observed that for $\varepsilon_{th} > 9$ ps, the *SINR* for PSWF is higher compared to MHP for the same n irrespective of c. The degradation of *SINR* with jitter was also found to be sharper in case of MHP compared to the graceful degradation for PSWF. On the other hand the *BEP* of MHP for all orders was higher than those of PSWF. It was also observed

from Figs 6 - 7 that *SINR* for PSWF wave-shapes with constant c reduces while *BEP* increases as the order n of pulse increases. On the other hand, for the same n the *SINR* for PSWF increases while *BEP* reduces as c increases. The above corroborates the variation of D_f with order and type of pulse shapes.

7. CONCLUSIONS

In this paper performance analysis of UWB signaling system using TH-PSM modulation scheme for a WPAN environment has been discussed. A frequency-considered selective multipath fading channel was in a multiple access scenario in the presence of timing jitter. The objective of performance analysis was to obtain higher *SINR* and lower *BEP* with respect to pulse shapes such as MHP and PSWF. The tolerance to timing jitter is compared for PSWF and MHP by
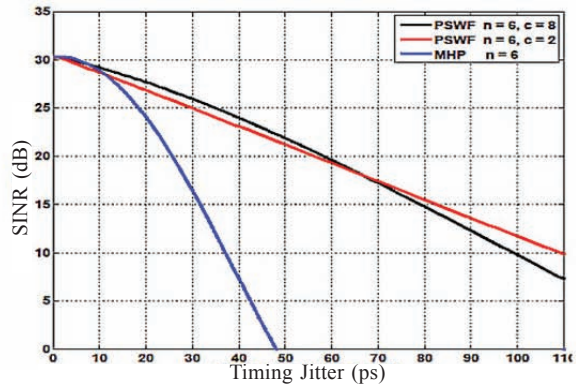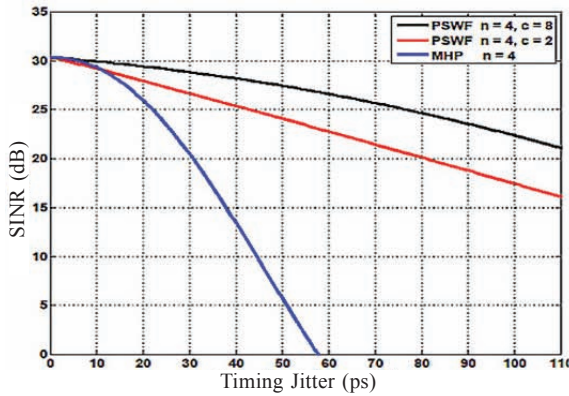

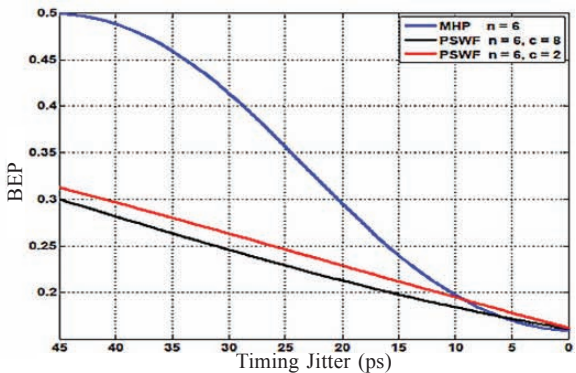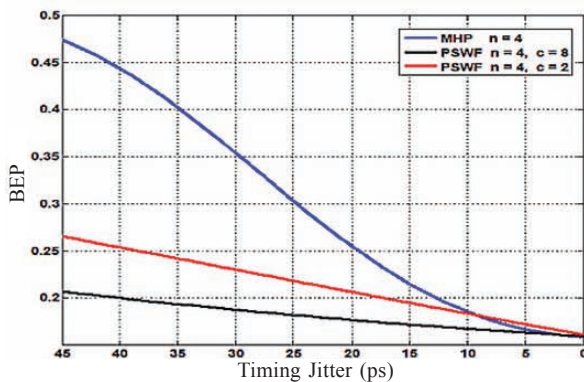**Figure 6.** SINR *vs* Jitter for MHP and PSWF of order n=4, 6 and c=2, 8.

Figure 7. BEP *vs* Jitter for MHP and PSWF of order $n = 4$, 6 and $c = 2$, 8.

introducing a new metric decision factor (D_f). It is demonstrated that in M-ary PSM scheme for the same value of timing jitter PSWF wave shapes yield a better SINR. Also for the same ACF, a higher upper bound of timing jitter exists for PSWF. This implies that PSWF wave shapes are more robust to timing jitter compared to MHP. This is also shown by the variation of *BEP* with respect to jitter. The receiver performance in terms of SINR is found to degrade rapidly for MHP as compared to PSWF with increase in timing jitter.

REFERENCES

1. Intel. Ultrawideband (UWB) Technology-enabling high-speed personal area networks. Intel Corporation, 2004.
2. Akbar, Rizwan; Radoi, Emanuel; Azou, Stéphane & Najam-ul-Islam, Muhammad. Low-complexity synchronization algorithms for orthogonally modulated IR-UWB systems. *EURASIP J. Wireless Commun. Networking*, 2013, **199**, 1-15. doi: 10.1186/1687-1499-2013-199
3. Lovelace & Townsend. The effects of timing jitter and tracking on the performance of Impulse. *IEEE J. Sel. Areas Commun.*, 2002, **20**(9), 1646-51. doi: 10.1109/JSAC.2002.805058
4. Rowe, D.; Pollack, B.; Pulver, J.; Chon, W.; Jett, P.; Fullerton, L. & Larson, L. A Si/SiGe HBT Timing Generator IC for High bandwidth Impulse Radio applications. *In* Proceedings IEEE Custom Integrated Circuits Conference, 1999. pp. 221-224. doi: 10.1109/cicc.1999.777278
5. Tian, Z & Giannakis. BER sensitivity to mistiming in ultra-wideband impulse radios. Part I: Non-Random channels. *IEEE Trans. Signal Proc.*, 2005, **53**(4),1550-1560. doi: 10.1109/TSP.2005.843747
6. Tian & Giannakis. BER Sensitivity to mis-timing in ultra-wideband impulse radios, Part II: Fading channels. *IEEE Trans. Signal Proc.*, 2005, **53**(5), 1897-1907. doi: 10.1109/TSP.2005.845485
7. Kokkalis, N.V. Performance analysis of M-ary PPM TH-UWB systems in the presence of MUI and timing jitter. *IEEE J. Sel. Areas Commun.*, 2006, **24**(4), 822-830. doi: 10.1109/JSAC.2005.863849
8. Nasr & Shaban. BER performance band data throughput of sinusoidal template-based IR-UWB receivers for WBAN. *Ame. J. Appl. Sci.,* 2013, **10**(5), 487-496. doi: 10.3844/ajassp.2013.487.496
9. Erb, S. & Pribyl, W. Design specifications for BER analysis methods using built-in jitter measurements. *IEEE Trans. VLSI Sys.*, 2012, **20**(10), 1804-1818. doi: 10.1109/TVLSI.2011.2163325
10. Gezici,; Molisch, Poor & Kobayashi. The tradeoff between processing gains of an impulse radio UWB system in the presence of timing jitter. *IEEE Trans. Comm.*, 2007, **55**(8), 1504-1515. doi: 10.1109/TCOMM.2007.902536
11. Usuda, K.; Zhang, H. & Nakagawa, M. M-ary pulse shape modulation for PSWF-based UWB systems in multipath fading environment. *In* Proceedings of IEEE Communications Society Globecom, 2004, 3498-3504. doi: 10.1109/glocom.2004.1379017
12. Majhi, Sudhan; Madhukumar, A.S.; Premkumar, A.B. & Richardson, Paul. Combining OOK with PSM modulation for simple transceiver of orthogonal pulse based TH-UWB systems. *EURASIP J. Wireless Comm. Networking*, 2008, 1-11. doi: 10.1155/2008/735410
13. Silva, J. & Campos. Spectrally efficient UWB pulse shaping with application in orthogonal PSM. *IEEE Trans. Comm.,* 2007, **55**(2), 313-22. doi: 10.1109/tcomm.2006.887493
14. Proakis. J. Digital communications. Mc Graw Hill, Ed 4th, 2001.
15. Win, M.Z. & Scholtz, R.A. Impulse radio: How it works. *IEEE Comm. Lett.*, 1998, **2**(2), 36-38. doi: 10.1109/4234.660796
16. Stuber, G. Principles of mobile communication. Ed 3, Springer, 2011. doi: 10.1007/978-1-4614-0364-7
17. FCC, First Report and Order, Federal Communications Commission, released 22 April, Washington D.C., 2002.
18. Adhikari, D & Bhattacharya, C. Analysis of power spectral density of ultra wideband waveforms for pulse shape modulation. *Int. J. Ultra Wideband Comm. Sys.*, 2014, **3**(1), 19- 30. doi: 10.1504/IJUWBCS.2014.060978

CONTRIBUTORS

Mr D. Adhikari is a BTech from Institute of Radio Physics and Electronics, University of Calcutta and ME from University of Pune. He is pursuing his PhD at the Defence Institute of Advanced Technology, Pune, India. Presently he is a Professor at the Symbiosis Institute of Technology, Pune.

Mr C. Bhattacharya is a Scientist in Defence Research and Development Organisation, India and Head of Department of Electronics Engineering in Defence Institute of Advanced Technology (DU), Pune, India. He has active interest in the broad areas of signal processing as radar, communication, genomics, imaging, etc. He has been awarded the *Best Researcher Award* from DIAT in May 2013 and *Technology Day Award* from Scientific Adviser in May 2014. He is a Senior Member of IEEE, USA.